

Segmentation of Brain Tumors in MRI Images Using Multi-scale Gradient Vector Flow

Anahita Fathi Kazerooni, *Student Member, IEEE*, Alireza Ahmadian*, *Senior Member, IEEE*, Nassim Dadashi Serej, Hamidreza Saligheh Rad, Hooshang Saberi, M.D, Hossein Yousefi, Parastoo Farnia

Abstract— The gradient vector flow (GVF) algorithm has been used extensively as an efficient method for medical image segmentation. This algorithm suffers from poor robustness against noise as well as lack of convergence in small scale details and concavities. As a cure to this problem, in this paper the idea of multi scale is applied to the traditional GVF algorithm for segmentation of brain tumors in MRI images. Using this idea, the active contour is evolved with respect to scaled edge maps in a multi scale manner. The edge detection performance of the modified GVF algorithm is further enhanced by applying a threshold-based edge detector to improve the edge map. The B-spline snake is selected for representation of the active contour, due to its ability to capture corners and its local control. The results showed an improvement of 30% in the accuracy of tumor segmentation against traditional GVF and 10% as compared to B-spline GVF in the presence of noise, besides the repeatability of the algorithm in contrast to traditional GVF. The clinical evaluation also proved the accuracy and sensitivity of the proposed method as 92.8% and 95.4%, respectively.

Keywords- Brain tumor segmentation, Multi scale GVF, traditional GVF, B-spline snake.

I. INTRODUCTION

Segmentation of brain tumors and reducing the user interaction are challenging issues, for which several approaches such as global thresholding, fuzzy-connectedness, Markov random fields (MRFs) [1-2] have been proposed. The active contours have also been applied extensively in several medical image segmentation applications. Among the existing active contours, level set methods have been used in brain tumor segmentation due to their ability in handling complex geometries [3]. However, they require adjustment of several parameters, which makes them user dependent. Also, they are performed in large number of iterations; thus, they are time consuming [4].

The other popular category of active contours, i.e. the parametric active contours or snakes are used to represent

the boundaries with elastic contours [5]. One of the assumptions in implementation of the snakes is that the region to be segmented is constructed from few numbers of non-overlapping structures. This limits the application of basic snakes in segmenting medical images, especially in brain tumor segmentation.

Several modifications have been made in designing the active contours, in order to make them appropriate in specific applications. One of such modifications was proposed by Xu and Prince [6], which is called “gradient vector flow (GVF) snake”. In the GVF method, a dense vector field is generated from the image by using vector diffusion, which guides the snake to fit a specific boundary [7]. The GVF snake has several advantages over the original snakes. For instance, the GVF snake is independent from the initial point. Also, it does not require prior knowledge about whether to inflate or deflate. Furthermore, in contrast to the original snake, in GVF method, the external force is not entirely irrotational. Thus, it can capture image concavities [6]. Therefore, GVF has become a popular method in medical image segmentation [8].

However, since the gradients are highly prone to noise, small scale details and tumor intensity inhomogeneity, the GVF external force is difficult to be handled in segmentation of tumors in brain MRI images [9]. Moreover, the evolution of the GVF snake is greatly dependent on the edge map created for it. For assuring the convergence of GVF snake, the edge map should be in such a way that while including all important edge information present in the image, it excludes the false edges created by lower intensity changes. In addition, the traditional GVF method requires selection of several parameters, which increases the time required for convergence [10].

In this work, the idea of multi-scale based GVF (MSGVF) snake is proposed to overcome the above problems with GVF snake. In this algorithm edge maps are updated in a multi-scale based approach which helps the gradient operator to deal with noise more efficiently.

Along with this multi-scale GVF, two modifications have also been made in order to improve the noise performance of the original GVF method, in detecting tumor boundaries. At first, the well known canny edge operator is applied in combination with upper and lower thresholds producing a threshold-based edge detector, by which false edges are eliminated and most of the prominent edges around the tumor area are detected. Secondly, a B-spline snake (or B-snake) is used in this paper to represent the active contour. The B-snake has significant advantages over the traditional snake, for example, it exhibits local control, it can capture

Manuscript received April 15, 2011.

* Corresponding Author: Alireza Ahmadian is with the Department of Biomedical Systems & Medical Physics, Tehran University of Medical Sciences, and Image Guided Surgery Lab, Research Center for Science and technology in Medicine (RCSTIM), Tehran, Iran; (corresponding author; e-mail: ahmadian@tums.ac.ir).

Anahita Fathi Kazerooni, Nassim Dadashi Serej, Hamidreza Saligheh Rad, Hossein Yousefi, and Parastoo Farnia are with the Department of Biomedical Systems & Medical Physics, Tehran University of Medical Sciences (TUMS), and Image Guided Surgery Lab, Research Center for Science and technology in Medicine (RCSTIM) Tehran, Iran;

Hooshang Saberi, MD, is with the Department of Neurosurgery, Imam Khomeini Hospital, Tehran University of Medical Sciences, and Brain and Spinal Injuries Repair Research Center (BASIR).

corners by allowing multiple knots, and its representation is compact [10].

In the next section, the MSGVF B-spline algorithm, for brain tumor segmentation is presented. This method is successfully performed on the brain MRI images with tumor conditions. The results are shown in section III, which show enhancement of tumor segmentation using the MSGVF B-spline approach. Finally, the discussion on the results is presented in section IV.

II. MATERIALS AND METHODS

A. Traditional active contours

A snake is a closed dynamic curve $r(s)=[x(s), y(s)]$, where s belongs to the interval $[0, 1]$ [5]. This curve is defined with two energy forces: internal energy, and external energy. These two energies work in opposition to each other. The total energy should be minimized, so that the snake converges to the object boundary.

$$E_{AC} = \int_0^1 \frac{1}{2} \left[\alpha |r'(s)|^2 + \beta |r''(s)|^2 \right] + E_{ext}(r(s)) ds, \quad (1)$$

where the first and second terms represent the internal and external energies of the snake, respectively. α and β are weighting parameters of elasticity and stiffness terms, and r' and r'' are the first and second derivatives of r with respect to s .

B. GVF Snake

The external energy in equation (1) can be defined by the gradient vector flow field. The GVF field is characterized by $z(x,y)=[u(x,y), v(x,y)]^T$ that minimizes the energy given by:

$$E_{GVF} = \iint \mu \left(|\nabla u|^2 + |\nabla v|^2 \right) + |\nabla f|^2 |z - \nabla f|^2 dx dy, \quad (2)$$

where f is the image edge map, μ is the smoothness degree, u and v are the components of the gradient vector in 2D space. The GVF snake performs poorly in segmenting the corners. Therefore, B-snake can be used to control the snake locally and reduce the number of parameters required for its representation.

C. B-snake and GVF

By using B-snake for contour representation, fewer points on the contour can be employed for evolution of the snake. Here, the cubic B-splines are used for this purpose. By uniform sampling, a set of control points $(CP_0, CP_1, \dots, CP_N)$ are sampled from the initial contour. Therefore, the initial active contour can be approximated by N cubic curve segments. The curve is defined by:

$$r(s) = \sum_{i=0}^{N-1} B_i(s) CP_i \quad (3)$$

where $B_i(s)$ are the B-spline basis functions and CP_i are the control points.

On each point (x_i, y_i) distributed uniformly around the spline, the GVF force can be denoted by $u(x_0, y_0), v(x_0, y_0)$. Thus the new points to be obtained after evolution can be computed by:

$$x_{i2} = x_{i1} + \eta u(x_{i1}, y_{i1}) \quad (4)$$

$$y_{i2} = y_{i1} + \eta v(x_{i1}, y_{i1})$$

The new sample points are used to compute new control points by minimizing the equation below:

$$\overline{CP}_{new} = \arg \min_{CP} \sum_{i=0}^{n-1} \left\| r(s_i) - \sum_{k=0}^{N-1} B_k(s_i) CP_k \right\| \quad (5)$$

where $\overline{CP} = (CP_0, CP_1, \dots, CP_{N-1})$.

D. Multiscale Gradient Vector Flow (MSGVF)

The GVF snake can become more robust to noise, small scale details and intensity inhomogeneity, by using the GVF in multi-scale stages [9]. This algorithm is based on scale space theory. The basic concept of scale space theory is generating a sequence of images $I_\sigma(x,y)$ from the initial image $I_0(x,y)$. As σ (scale) increases, $I_\sigma(x,y)$ becomes a coarser version of the image obtained in the previous stage [11].

In each scale, the resulting smoothed image from the previous stage is lowpass filtered and the threshold-based edge map of this image is computed. The threshold is applied due to the generation of various edges around the tumor, among which false edges are also present due to inhomogeneity in image intensities and noise. The value of the upper threshold was chosen for dealing with the edges caused by noise and large image gradients. However, the lowpass filtering and using the upper threshold causes the edges to become blurred, thus, their detection and localization becomes difficult [11]. Therefore, the lower threshold is selected considering the intensities on tumor boundary, in order to preserve the important edges.

Here, the edge map is computed using Gaussian smoothing filters and threshold-based canny edge detector. The Gaussian filter used for the scale generation is defined as:

$$h_\sigma(x,y) = \frac{1}{2\pi\sigma^2} e^{-\frac{(x^2+y^2)}{2\sigma^2}} \quad (6)$$

where σ (the standard deviation of the Gaussian filter) denotes the scale. The smoothed image in each scale can be acquired by the convolution of the smoothing filter with the image obtained in previous scale:

$$I_{\sigma_i}(x,y) = h_{\sigma_i}(x,y) * I_{\sigma_{i-1}}(x,y) \quad (7)$$

The multiscale edge map is computed by taking the laplacian of the smoothed image:

$$f_{\sigma_i}(x,y) = |\nabla I_{\sigma_i}(x,y)| \quad (8)$$

The final result can be inserted in equation (2) to compute the external force of the GVF snake. The number of scales is selected to be 5. The Gaussian filter is applied in each scale with standard deviations equal to $\sigma = 3, 15, 31, 63, \text{ and } 127$. In fact, the ability of changing the smoothing window size in multi-scale approach has led to precisely aligning the gradient map according to the true edges appeared in tumor boundaries. As it can be observed from Fig.1, the gradient

vectors become in alignment with tumor boundaries by increasing the scale.

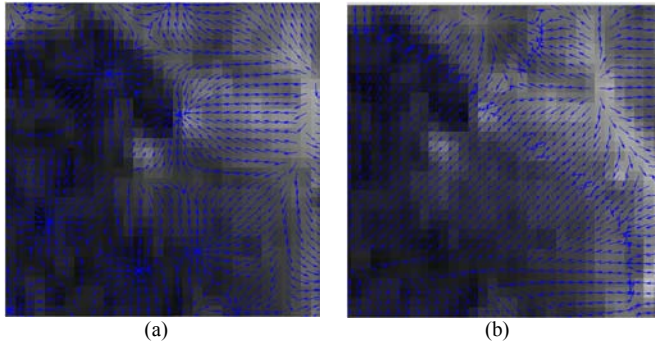


Fig. 1. The GVF of a part of tumor boundary in different scales: (a) scale 1 ($\sigma=3$), and (b) scale 5 ($\sigma=127$). The figure shows the alignment of gradient vectors (in blue) with tumor borders over scale.

The initial contour for the GVF snake is selected manually, which is updated in each of the proceeding scales. The GVF B-snake deformation initializes from the position of control points reached in the previous scale. The segmentation is completed after 40 iterations.

E. MR Dataset

The datasets used for this work are adopted from Surgical Planning Laboratory at Harvard Medical School website (www.spl.harvard.edu/). The images are taken from patients with “Oligoastrocytoma” and “glioblastoma” brain tumors, acquired on a 1.5T scanner. The resolution of the images is 256x256 with 120 or 90 slices (depending upon each dataset). The voxel resolution is $1 \times 1 \times 1.5 \text{ mm}^2$. An example of one of the datasets with Oligoastrocytom pathology is shown in Fig.2.

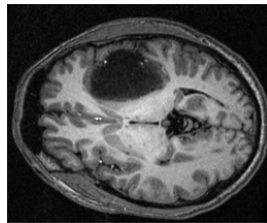


Fig. 2. Axial cross section of T1-weighted MRI from a case with tumor in left perisylvian region of brain.

III. RESULTS

The MSGVF B-Spline was successfully applied on the datasets and compared to the manual segmentation performed by an expert rater. The algorithm was run on individual slices containing tumor.

The result of applying the MSGVF B-spline snake in comparison with the MSGVF with traditional snake is shown in Fig.3.

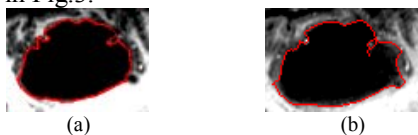


Fig. 3. The result of applying (a) MSGVF B-spline algorithm, and (b) MSGVF with traditional snake on one of the slices of case 1. As it can be observed the B-spline snake performs superior to the traditional snake in capturing the corners.

This figure illustrates the ability of B-snake in capturing

the corners, which is due to the local control of B-snakes and the feasibility of selecting knots. Therefore, here the results of MSGVF with B-snake knots are considered for further analysis on the performance of multi scale method.

As mentioned previously, the MSGVF is meant to be more robust against noise and intensity inhomogeneity in contrast to traditional GVF. Therefore, salt and pepper type of noise with intensity in the range of 0.01- 0.03 was added to the images in order to examine the performance of the MSGVF B-spline algorithm. This type of noise was chosen because it produces high variations in the gradients of the image. As GVF segmentation method is highly dependent on gradients of the image, the gradients can be trapped by the edges created by this type of noise. Thus, it can best examine the performance of gradient operator in edge detection during the curve evolution. The effects of applying the MSGVF B-spline with Gaussian kernel in various scales in the presence of noise are shown in Fig. 4.

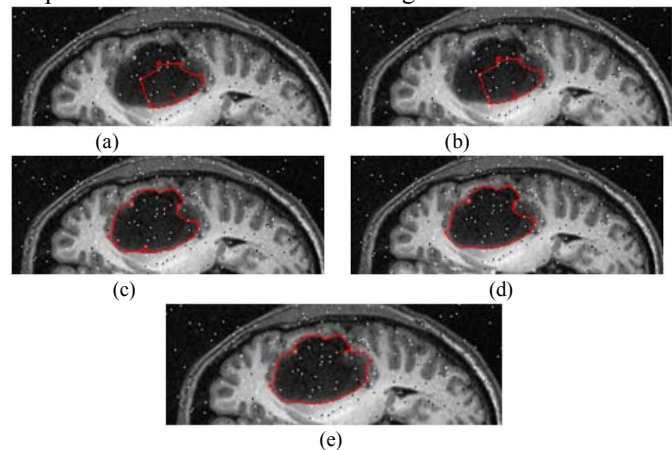


Fig. 4. The performance of the MSGVF algorithm with Gaussian filter in presence of noise (with intensity= 0.01). The segmented part is shown in red. The result in (a) scale 1 ($\sigma=3$), (b) scale 2 ($\sigma=15$), (c) scale 3 ($\sigma=31$), (d) scale 4 ($\sigma=63$), and (e) scale 5 ($\sigma=127$).

As it is apparent from Fig.4, the performance of MSGVF with Gaussian smoothing filter in the presence of noise is highly improved over the subsequent scales. The visual inspection of the result of Fig. 4(d) shows the ability of the proposed method in tumor segmentation. These results were evaluated qualitatively by comparing manual segmentation carried out by an expert radiologist with the outcome of the algorithm in each scale. Then, the resulting sensitivity and accuracy for one of the datasets were calculated to represent the evaluation, which are summarized in Table I.

TABLE I
THE VALIDATION RESULTS FOR COMPARING THE PERFORMANCE OF THE ALGORITHM OVER SCALE

Scale No.	Accuracy (%)	Sensitivity (%)
scale 1	62.04	23.64
scale 2	71.14	46.3
scale 3	75.05	58.91
scale 4	79.38	71.82
scale 5	87.38	92.81

Fig.5 illustrates the comparison of applying Traditional GVF, Bspline GVF, and MSGVF Bspline procedures in detecting the boundaries of tumor when noise is added.

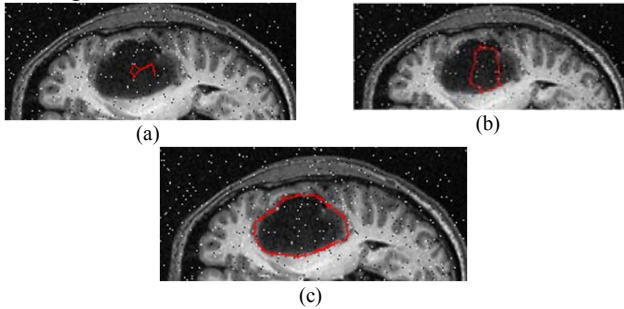


Fig. 5. The comparison between the results of applying (a) Traditional GVF, (b) Bspline GVF, and (c) MSGVF Bspline algorithms, in the presence of noise (intensity=0.02) on detecting the tumor borders.

As it is apparent from Fig.5, the MSGVF Bspline algorithm has shown a degree of robustness in the presence of noise and small scale details.

The quantitative comparison of the performance of the three algorithms which is averaged for the three datasets is presented in Table II. In addition, the time required for each algorithm to converge is shown in the last column.

TABLE II
THE VALIDATION RESULTS FROM VARIOUS METHODS

Algorithm	Accuracy (%)	Sensitivity (%)	Time (sec)
Traditional GVF	59.95	12.88	7.2
BSpline GVF	80.68	63.14	3.6
Multiscale Bspline GVF	92.8	95.4	15.2

As it is apparent from the outcome of Table II, the MSGVF Bspline exhibits significant improvement over the traditional and Bspline GVFs. As discussed earlier, the Bspline snake needs less time to converge due to its compact representation in comparison with the traditional snake. However, the MSGVF Bspline is performed in longer duration than the other two methods, due to being processed in a sequence of scales.

The outcome of several runs of the algorithms in the presence of salt and pepper noise showed that the boundary segmented by MSGVF Bspline method was retained at each time, in contrast to the traditional and Bspline GVF snakes. This illustrates the relative insensitivity of MSGVF Bspline algorithm to random noise. Therefore, this approach is found repeatable in various conditions in comparison with traditional and Bspline GVF.

IV. CONCLUSION

The performance of traditional GVF method degrades in segmenting brain tumors in noisy MRI images, due to the complexity of the shape of the brain tumors (such as small scale details). The proposed method was found robust in detecting tumor boundaries, in the presence of noise, intensity variations and small scale details. This happens because in the scale space, in finer levels the region consists of a number of small details including outliers. In higher or

coarser scales, the small details are merged to form larger regions [11]. This process while preserving small details, handles the large variations in image gradients.

This algorithm appeared more robust compared to the traditional GVF and Bspline GVF. The Bspline snake employed as the active contour improves the algorithm to capture corners and to reduce the computation. It also gives the opportunity to locally control the snake by changing the knots. The threshold-based edge detector enhanced the performance of true edge detection by reducing false positive rates caused by intensity changes and noise. Ultimately, the multi scale GVF Bspline method outperforms the traditional and Bspline GVF methods by about 30% and 10% improvement in accuracy, respectively.

However, applying MSGVF algorithm to segment tumors in brain images requires selecting an initial contour due to presence of small structures and inhomogeneity of the brain images. This can become less problematic by changing the upper and lower values of the edge threshold and changing the type of the edge detector.

We are currently working on enhancing the robustness of the algorithm in high noise environments, optimizing the method by changing the algorithm of edge map generation, and on making this segmentation method completely automatic to aid neurosurgeons in segmenting the desired structures as a pre-processing step in image guided surgery systems.

ACKNOWLEDGMENT

This work was credited by grant no. 89-04-30-11992, Faculty of Medicine, Tehran University of Medical Sciences, Tehran, Iran. We would like to deeply acknowledge RCSTIM for providing invaluable resources.

REFERENCES

- [1] L. M. Fletcher-Heath, *et al.*, "Automatic segmentation of non-enhancing brain tumors in magnetic resonance images," *Artificial Intelligence in Medicine*, vol. 21, pp. 43-63, 2001.
- [2] L. Clarke, *et al.*, "MRI segmentation: methods and applications," *Magnetic resonance imaging*, vol. 13, pp. 343-368, 1995.
- [3] R. Dubey, *et al.*, "Semi-automatic Segmentation of MRI Brain Tumor," *ICGST-GVIP Journal*, vol. 9, pp. 33-40, 2009.
- [4] S. Taheri, *et al.*, "Level-set segmentation of brain tumors using a threshold-based speed function," *Image and Vision Computing*, vol. 28, pp. 26-37, 2010.
- [5] L. He, *et al.*, "A comparative study of deformable contour methods on medical image segmentation," *Image and Vision Computing*, vol. 26, pp. 141-163, 2008.
- [6] C. Xu and J. L. Prince, "Snakes, shapes, and gradient vector flow," *Image Processing, IEEE Transactions on*, vol. 7, pp. 359-369, 1998.
- [7] H. Park and M. Chung, "A new external force for active contour model: virtual electric field," 2002, pp. 103-106.
- [8] C. Xu, *et al.*, "Image segmentation using deformable models," *Handbook of Medical Imaging, Medical Image Processing and Analysis*, vol. 2, pp. 129-174.
- [9] J. Tang and S. T. Acton, "Vessel boundary tracking for intravital microscopy via multiscale gradient vector flow snakes," *Biomedical Engineering, IEEE Transactions on*, vol. 51, pp. 316-324, 2004.
- [10] P. Brigger, *et al.*, "B-spline snakes: A flexible tool for parametric contour detection," *Image Processing, IEEE Transactions on*, vol. 9, pp. 1484-1496, 2000.
- [11] P. Perona and J. Malik, "Scale-space and edge detection using anisotropic diffusion," *Pattern Analysis and Machine Intelligence, IEEE Transactions on*, vol. 12, pp. 629-639, 1990.